Received: 25 May 2020 | Revised: 11 July 2020 | Accepted: 21 July 2020

DOI: 10.1002/chir.23275

WILEY

REGULAR ARTICLE

Multifunctional chiral aminophosphines for enantiodivergent catalysis in a palladium-catalyzed allylic alkylation reaction

Sviatoslav S. Eliseenko[1] | **Mohan Bhadbhade**[2] | **Fei Liu**[1]

[1]Department of Molecular Sciences, Macquarie University, Sydney, New South Wales, Australia

[2]Solid State & Elemental Analysis Unit, Mark Wainwright Analytical Centre, Division of Research, The University of New South Wales, Sydney, New South Wales, Australia

Correspondence
Fei Liu, Department of Molecular Sciences, Macquarie University, Sydney, New South Wales, Australia.
Email: fei.liu@mq.edu.au

Funding information
Macquarie University, Grant/Award Numbers: iMQRES award (2015071), 2015071

Abstract

Trifunctional MAP-based chiral phosphines were tested as new ligands in a Pd-catalyzed asymmetric allylic alkylation, demonstrating fast and enantiodivergent catalysis. The palladium complexes of representative ligands by X-ray analysis revealed a novel mode of *P*,*N*-coordination of the ligand to the palladium center, which may contribute to switching the sense of the asymmetric induction via combined steric and tunable H-bonding interactions between the metal complex and the substrates.

KEYWORDS

catalytic dualism, enantiodivergent catalysis, H-bonding ligands

1 | INTRODUCTION

Chiral compounds are essential in chemical research, and asymmetric catalysis remains the main avenue for efficiently accessing chiral compounds. While a high-performing chiral catalyst can readily enable reaction conversion with the preferred sense of asymmetric induction, a more versatile goal is to achieve enantiodivergent or stereodivergent asymmetric catalysis in which the sense of asymmetric induction can be switched to access either enantiomeric product without changing the catalyst's initial chirality.[1] This atom economic mode of asymmetric catalysis, however, is also very challenging in reaction design in both metal-catalyzed and organocatalyzed processes. Interestingly, given that the combination of metal catalysis and organocatalysis is a rapidly developing field,[2–4] in which an organocatalyst can serve as either a catalyst or a ligand, exploring enantiodivergent catalysis in this hybrid mode of catalysis may present new opportunities in finding cooperative catalytic modes. Here, we report an enantiodivergent catalysis in a Pd-catalyzed asymmetric allylic alkylation (AAA) reaction, induced by a multifunctional chiral phosphine ligand. The novel chelation mode of Pd to the *P*,*N*-ligand, as shown by X-ray analysis, suggested potential cooperativity in substrate activation and direction, from tuning hydrogen-bonding interactions within the multifunctional ligand coordinated to the palladium center, for switching the sense of the asymmetric induction in the reaction even when the chirality of the ligand remained unchanged.

In combined metal-catalysis/organocatalysis, the dominant concepts include the cooperative mode (both types of catalysts participate in the same catalytic cycle), the synergistic mode (distinct metal-catalytic and organocatalytic cycles in cooperation), and the sequential or relay mode (two detached catalytic cycles are performed in a consecutive manner through the formation of an intermediate).[3] The use of one chiral structure as a ligand and a catalyst may improve both catalytic

compatibility and cooperativity in the cooperative mode. Despite the simplicity of the idea, an efficient combination of organocatalytic and metal-ligating properties in a structure (catalytic dualism) is challenging with only limited examples known from carbene-,[5,6] urea-,[7] and pyrrolidine-containing structures,[8] *N*,*N*′-dioxides,[9] aminophosphines,[10–20] and 1,4-hydroxyarylalcohols (also known as HAROLs).[21] Therefore, one current challenge is to design catalytic roles with a more complex organization in the reaction environment to enable not just efficient asymmetric catalysis but also dynamic properties such as catalytic dualism and chiral induction switching.

Ligands with H-bonding properties are excellent candidates for designing more organized catalysis, and existing H-bonding ligands may be broadly classified into two different approaches of substrate recruitment. The first "ligand–substrate" approach is provided by ligands with metal-binding fragment and an H-bonding moiety, located in a remote position away from the metal center (Figure 1A). This strategy allows the binding of a specific substrate by a certain H-bonding moiety of the ligand through a set of weak interactions in order to orient the substrate's reactive site to the coordinated metal center selectively. This approach was successfully applied in a series of highly enantioselective processes (mostly >95% *ee*) such as Pd-catalyzed allylic substitution[22,23] (including enantiodivergent examples),[24–28] Mn-sulfoxidation,[29] Ru-epoxidation,[30] Pd-arylation and vinylation,[31,32] and Rh-hydrogenation.[33–37]

The second acceptor-type "metal–ligand–substrate" strategy is provided by a ligand where its metal-binding fragment also serves as an H-bonding acceptor in close proximity to the metal coordination site. This strategy allows the formation of a planar pseudo cycle (Figure 1B) and is mostly applied in aldehyde recruitment.[38–40] The coordination of the aldehyde oxygen to boron or titanium enhances the electron density on the ligand's oxygen atom attached to the Lewis acid. It makes the oxygen atom more susceptible to form the H-bond with the formyl hydrogen where the positive charge is increased due to the coordination. The five-membered cycle formed keeps the aldehyde in a specific position that favors enantioselective outcomes in allylation, aldol, Diels-Alder, hydrocyanation, and ene reactions.[38–40]

In this work, a new type of metal–ligand–substrate donor-type ligands is investigated (Figure 1C). These ligands are multifunctional chiral phosphines, studied as trifunctional organocatalysts in our previous works[41–48] that have demonstrated proficient catalysis in Morita–Baylis–Hillman model reactions. Our trifunctional system, which combines catalytic motifs such as phosphine Lewis base, amine Brønsted base, and phenol or sulfonamide Brønsted acid, can now be tested for its ability to provide potential metal-coordination sites and H-bonding interactions concurrently for dual activation in a model Pd-catalyzed allylic alkylation. The multifunctional chiral phosphine may act as a ligand to the metal and also organize H-bonding interactions for synergistic substrate direction. While trifunctional or multifunctional catalysts are seeing wider applications in organocatalytic reactions[49–51] here we demonstrate the application of multifunctional catalysts in metal-catalyzed processes.

We used the well-established Pd-catalyzed AAA to test the applicability of our multifunctional chiral phosphines as ligands as well as H-bonding activators, with the phosphine center as the expected metal coordination site.[24–28] We found that trifunctional MAP-based ligands provide unusual *P*,*N*-coordination sites for the palladium center. The tuning of the trifunctional ligand's Brønsted acid motif resulted in responses from both the enantioselectivity and reaction rate. Further alteration of the Brønsted acid type allowed switching of the sense

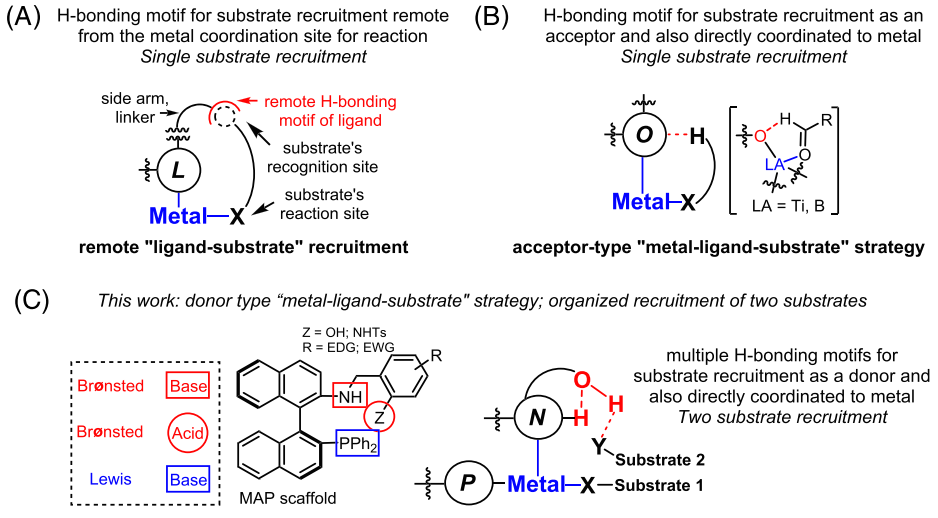

FIGURE 1 (A and B) Types of known H-bonding ligands in metal-catalyzed reactions. (C) Proposed catalytic dualism by the MAP-based trifunctional system in H-bonding-assisted metal-catalysis with more organization

of the asymmetry induction and demonstrated the ability of the trifunctional MAP system to provide enantiodivergent catalysis.

2 | MATERIALS AND METHODS

2.1 | General information

All reagents unless specified are commercially available and purified by standard procedures.[52] Deuterated solvents were purchased from Cambridge Isotope Laboratories, USA. Potassium carbonate, potassium acetate, and BSA were used in a glovebox under nitrogen atmosphere. Air and moisture sensitive reactions were performed under nitrogen or argon atmosphere. Flash column chromatography was performed on Merck silica gel 60 (0.015–0.040 mm). ^{1}H, ^{13}C, and ^{31}P experiments were performed at 298 K on a Bruker DPX 400-MHz spectrometer equipped with a 5-mm QNP probe. Chemical shifts were reported in ppm using the residual $CHCl_3$ (δ_H = 7.26 ppm, δ_C = 77.16 ppm) or CH_2Cl_2 (δ_H = 5.32 ppm, δ_C = 53.8 ppm) peaks as an internal reference. All ^{31}P NMR spectroscopy was performed on a Bruker DPX 400-MHz spectrometer at 298 K, and all spectra were referenced to external H_3PO_4 (0 ppm). All spectra were processed using Bruker TOPSPIN software versions 4.0.7. High-resolution mass analysis was provided by the Australian Proteome Analysis Facility (APAF), Macquarie University, Sydney, Australia. High-performance liquid chromatography (HPLC) analysis was performed using a Shimadzu Prominence system with CHIRALPAK® AD–H column. HPLC grade solvents were degassed before use. The X-ray diffraction measurements were carried out on a Bruker D8 Quest Single Crystal diffractometer with Photon II detector at 150 K by using IμS 3.0 microfocus source with Mo-Kα radiation (λ = 0.710723 Å). Starting acetate **6** was synthesized by a known procedure.[53]

2.2 | Experimental details

2.2.1 | General procedure for Pd-catalyzed AAA (diethylzinc conditions)

Ligand (3.0 μmol) and palladium (II) dichloride diprop-2-en-1-ide (0.73 mg, 2.0 μmol) were placed in a 2-ml amber, oven-dried vial ("catalyst" vial) as stock solutions in freshly distilled dioxane. The volume of dioxane was adjusted to 150 μl and the mixture left to stir for 40 min at room temperature. Acetate **8** (10 mg, 40 μmol) was then added into the vial as a solution in dioxane and the mixture left to stir for 10 min more at room temperature. Dimethyl malonate (9.1 μl, 80 μmol) was placed in a separate 2-ml amber, oven-dried vial ("nucleophile" vial), diluted with 100 μl of dioxane, and cooled down in an ice bath. Then diethylzinc (9.8 mg, 80 μmol) as 1 M solution in hexanes was slowly added into the nucleophile vial with stirring and the volume of dioxane was adjusted to 600 μl. Then, the cold mixture from the nucleophile vial was transferred slowly into the catalyst vial. The nucleophile vial was rinsed with 100 μl of dioxane twice, and the resulting solution was added to the catalyst vial. The mixture (final volume ~1 ml) was left to stir at room temperature for 48 h. Then, the reaction mixture was diluted with ethyl acetate and quenched with a saturated ammonium chloride solution. The aqueous layer was extracted with ethyl acetate twice, and the combined organic layer was washed with brine, dried over sodium sulfate, and concentrated by nitrogen flow to yield dimethyl-2-(1,3-diphenylallyl)malonate **9** and reduction product **10**.

2.2.2 | General procedure for Pd-catalyzed AAA (BSA conditions)

Ligand (3.0 μmol) and palladium (II) dichloride diprop-2-en-1-ide (0.73 mg, 2.0 μmol) were placed in a 2-ml amber, oven-dried vial (catalyst vial) as stock solutions in freshly distilled dichloromethane. The volume of dichloromethane was adjusted to 100 μl and the mixture left to stir at room temperature for 1 h. Potassium carbonate (0.41 mg, 3.0 μmol) was placed in a separate 2-ml amber, oven-dried vial (nucleophile vial) in a glovebox under nitrogen atmosphere following by the addition of 100 μl of dichloromethane, BSA (29 μl, 119 μmol), and dimethyl malonate (14 μl, 119 μmol). The volume was adjusted to 250 μl and the mixture left to stir at room temperature for 1 h. Acetate **8** (10 mg, 40 μmol) was added into the catalyst vial as a solution in dichloromethane and the mixture left to stir for 0.5 h more at room temperature. Then, the mixture from the catalyst vial was transferred slowly into the nucleophile vial. The catalyst vial was rinsed with 100 μl of dichloromethane twice, and the resulting solution was added to the nucleophile vial and the mixture (final volume 500 μl) left to stir at room temperature for an indicated time. During the reaction time, 30-μl aliquots were taken at 0.5, 1.5, 3, and 6 h for the conversion and enantioselectivity analysis. Then, the reaction mixture was dissolved in ethyl acetate and treated with saturated ammonia chloride solution. The aqueous layer was extracted with ethyl acetate twice, and the combined

organic layer was washed with brine, dried over magnesium sulfate, filtered, and concentrated by nitrogen flow to yield dimethyl-2-(1,3-diphenylallyl)malonate **9**. A pure product sample for characterization was obtained by purification of the crude mixture on a silica gel pipette column (gradient hexanes/ethyl acetate).

2.2.3 | Ligand 6

Aminophosphine **7** (49 mg, 0.11 mmol) was placed into a dry 4-ml amber HPLC vial with a septum in a glovebox under nitrogen atmosphere; then, the vial was removed from the glovebox, and 0.3 ml of freshly distilled 1,2-dichloroethane was added under argon environment. Neat distilled *p*-methoxy benzaldehyde (29 mg, 0.22 mmol) and acetic acid (16 mg, 0.27 mmol) were added, and the mixture left to stir at room temperature for 3.5 h, then cooled down by ice bath, and sodium triacetoxyborohydride (85 mg, 0.40 mmol) was added in one portion. The mixture was left to stir at room temperature for another 40 min and cooled down in an ice bath. Sodium tetrahydroborate (33 mg, 0.86 mmol) was then added in one portion. The mixture was left to stir at room temperature for 25 min and cooled down in an ice bath, and 1-ml MiliQ water was added slowly to the reaction mixture. The mixture was transferred to a separating funnel and extracted with DCM three times. The combined organic layer was treated with brine, dried over magnesium sulfate, and concentrated under a nitrogen flow. The crude mixture was purified by column chromatography (gradient hexanes/ethyl acetate) yielding product **6** in 25 mg (41% yield). ^{1}H NMR (400 MHz, $CDCl_3$) δ 3.64 (br. s., 1H), 3.74 (s, 3H), 3.96 (dd, J = 4.3, 15.3 Hz, 1H), 4.07–4.18 (m, 1H), 6.60 (d, J = 8.5 Hz, 1H), 6.70 (d, J = 8.7 Hz, 2H), 6.89–6.95 (m, 1H), 6.98 (d, J = 8.6 Hz, 2H), 7.02–7.11 (m, 4H), 7.12–7.38 (m, 10H), 7.44–7.55 (m, 2H), 7.71 (d, J = 8.0 Hz, 1H), 7.82 (d, J = 8.6 Hz, 1H), 7.88 (d, J = 8.5 Hz, 1H), 7.89 (d, J = 8.1 Hz, 1H); ^{13}C NMR (100 MHz, $CDCl_3$) δ 47.27, 55.35, 113.73, 113.90, 116.16 (d), 121.62, 124.23, 126.17, 126.66 (d), 126.91, 127.13, 127.26, 127.92, 128.09, 128.20, 128.26, 128.33, 128.49, 128.55, 129.64, 130.87 (d), 131.85, 133.08 (d), 133.53, 133.59, 133.73, 133.79, 134.21 (d), 134.36, 137.61, 137.74 (d), 138.16, 138.30, 141.76, 142.11, 143.85 (d), 158.61; ^{31}P NMR (162 MHz, $CDCl_3$) δ −14.21; IR (ATR, cm^{-1}) ν 3,426, 3,050, 2,927, 1,742, 1,616, 1,597, 1,510, 1,430, 1,339, 1,299, 1,244, 1,172, 1,151, 1,093, 1,027, 953, 915, 808, 773, 739, 695, 628; high-resolution mass spectrometry (HRMS) (electrospray ionization [ESI], *m/z*): $[M + H]^+$, calcd. for $C_{40}H_{33}NOP$ 574.22997; found, 574.22914; $[\alpha]_D^{20} = +33.81^\circ$ (*c* 1.0, $CHCl_3$).

2.2.4 | Complex Pd/1

A solution of ligand **1** (31.8 mg, 56.82 μmol) in 0.57 ml of degassed dry dichloromethane was added bis(benzonitrile)palladium (II) chloride (21.79 mg, 56.82 μmol) over argon. The reaction was stirred for 5 min at room temperature in an inert atmosphere providing a suspension. The precipitate was filtered out and washed with dichloromethane, providing 17 mg (41% yield) of the desired product as a yellow solid. The precipitate was dissolved in 0.9 ml of degassed dichloromethane and filtered through KimVap into a 2 ml clear HPLC vial. Then, 0.3 ml of degassed hexane was added to the solution through a KimVap filter. The resulting solution was shaken to mix the solvent layers and left in a fridge for slow evaporation. After 6 days, yellow crystals of compound Pd/**1** were formed. ^{1}H NMR (400 MHz, CD_2Cl_2, δ) 3.92 (br. s, 1H), 4.66 (dd, J = 14.5, 2.9 Hz, 1H), 4.82 (dd, J = 14.5, 9.9 Hz, 1H), 5.71 (d, J = 8.0 Hz, 1H), 6.22 (d, J = 8.4 Hz, 1H), 6.24 (br.s, 1H), 6.28 (d, J = 8.6 Hz, 1H); 6.54 (td, J = 7.5, 0.9 Hz, 1H), 6.74–6.89 (m, 6H), 6.94–7.00 (m, 1H), 7.13–7.19 (m, 1H), 7.25 (t, J = 8.5 Hz, 1H), 7.48–7.64 (m, 8H), 7.96–8.04 (m, 3H), 8.20 (d, J = 9.0 Hz, 1H); ^{13}C NMR (100 MHz, CD_2Cl_2, δ) 54.03, 115.47, 120.47, 121.09, 121.24, 123.89, 124.36, 124.95, 125.34, 125.80, 126.43, 126.50, 126.92, 128.02, 128.24, 128.29, 128.41, 128.51, 128.60, 128.71, 128.78, 128.85, 128.88, 128.95, 130.03, 130.28, 130.35, 131.35, 131.65, 131.72, 131.80, 131.93, 132.02, 134.00, 134.79, 135.58, 138.92, 139.86, 153.42; ^{31}P NMR (162 MHz, CD_2Cl_2, δ) 24.97; IR (ATR, cm^{-1}) ν 3,222, 3,054, 2,918, 1,595, 1,502, 1,456, 1,436, 1,337, 1,261, 1,227, 1,184, 1,099, 1,028, 995, 894, 869, 817, 746, 688, 628; UV (λ_{max}, nm [ε, M^{-1} cm^{-1}]): 278 [21,534], 292 [18,022], 320 [9,231], 350 [4,423]; HRMS (ESI, *m/z*): $[M - Cl]^+$ calcd. for $C_{39}H_{30}ClNOPPd$ 700.07828; found, 700.07848; $[\alpha]_D^{25} = -461.93^\circ$ (*c* 0.4, CH_2Cl_2).

2.2.5 | Complex Pd/5

A solution of ligand **5** (37.5 mg, 526 μl, 52.6 μmol) in 0.53 ml of degassed dry dichloromethane was added bis(benzonitrile)palladium (II) chloride (20.18 mg, 52.6 μmol) over argon. The reaction was stirred for 5 min at room temperature in an inert atmosphere and then filtered through KimVap and washed with dichloromethane. Degassed hexane was added to the solution to form a double-layer mixture that left to stay overnight. Next morning, the clusters of yellow solid formed on the bottom of the vial. The clusters were filtered out, providing 31.4 mg (67% yield) of the desired product. The aliquot of solid was dissolved in 0.9 ml of

degassed dichloromethane and filtered through KimVap into a 2-ml clear HPLC vial. Then, 0.3 ml of degassed hexane was added to the solution through KimVap filter. The resulted solution was shaken to mix the solvent layers and left in a fridge for slow evaporation. After 3 days, yellow crystals of compound Pd/**5** were formed. ^{1}H NMR (500 MHz, $CDCl_3$, δ) 2.34 (s, 3H), 5.01 (dd, J = 14.5, 10.0 Hz, 1H), 5.11 (dd, J = 14.5, 2.0 Hz, 1H), 5.93 (d, J = 7.7 Hz, 1H), 6.02 (d, J = 8.4 Hz, 1H), 6.51 (s, 1H), 6.55–6.63 (m, 3H), 6.70–6.85 (m, 8H), 6.95–7.02 (m, 3H), 7.14–7.20 (m, 1H), 7.25–7.31 (m, 1H), 7.44–7.61 (m, 7H), 7.67 (d, J = 8.1 Hz, 1H), 7.83 (d, J = 8.8 Hz, 1H), 7.89 (d, J = 7.8 Hz, 1H), 8.08 (d, J = 9.0 Hz, 1H), 8.46 (d, J = 9.0 Hz, 1H); ^{13}C NMR (100 MHz, $CDCl_3$, δ) 21.73, 52.16, 118.92, 118.88, 121.34, 124.14, 125.39, 125.95, 126.33, 126.66, 127.10, 127.65, 127.98, 128.07, 128.10, 128.31, 128.53, 128.81, 129.22, 129.41, 129.55, 129.64, 130.84, 130.86, 131.18, 131.64, 131.77, 131.89, 131.90, 133.14, 133.22, 134.63, 134.65, 134.67, 134.83, 135.34, 135.54, 135.66, 138.59, 139.85, 143.49; ^{31}P NMR (162 MHz, $CDCl_3$, δ) 23.56; IR (ATR, cm^{-1}) ν 3,055, 2,956, 2,918, 2,850, 1,717, 1,596, 1,455, 1,437, 1,377, 1,329, 1,260, 1,184, 1,158, 1,093, 1,021, 892, 868, 812, 744, 687; UV (λ_{max}, nm [ε, M^{-1} cm^{-1}]): 294 (15,346), 319 (7,355); HRMS (ESI, m/z): $[M - Cl]^+$ calcd. for $C_{46}H_{37}ClN_2O_2PPdS$ 853.10312; found, 853.10308; $[\alpha]_D^{25} = -137.3°$ (c 0.5, CH_2Cl_2).

3 | RESULTS AND DISCUSSION

3.1 | Synthesis of ligands

A set of trifunctional ligands **1**–**5**, synthesized by reported earlier procedures,[45,47,48] and a control ligand **6** were tested in palladium-catalyzed AAA. The late-stage precursor (*S*)-MAPO was synthesized from commercially available (*S*)-BINOL via Buchwald–Hartwig amination (amine insertion) and triflate–phosphine oxide coupling (phosphine insertion) in 46% yield over 10 steps (Scheme 1A). The final multidentate ligands **1**–**6** can be further obtained from (*S*)-MAPO in two steps via phosphine oxide reduction and reductive amination of a corresponding aromatic aldehyde (Brønsted acid insertion) (Scheme 1B). The different acidities of H-bonding motifs in ligands **1**–**4** may influence enantioselectivity of the reaction as observed earlier for organocatalysis.[45,47] Ligands **2** and **4** bearing bulky *tert*-butyl groups in different positions were tested for assessing the potential steric requirements on the reaction outcome. Ligand **5** has a tosylamide Brønsted acid motif that significantly differs from the phenolic moiety in ligands **1**–**4** and may alter the level and sense of the asymmetric induction. Ligand **6** does not have an H-bonding fragment and was synthesized as a control ligand. (NMR spectra of ligand 6are provided in Supporting Information).

3.2 | Palladium complexation: Novel metal–ligand–substrate donor-type *P,N*-mode

In the seminal investigations of palladium coordination on 2-dimethylamino-2′-diphenylphosphino-1,1′-binaphthyl (MAP) ligand, Kocovsky et al.[54] and Ding et al.[55] described the predominant formation of P, C_σ-complexes (Figure 2A). The further partial reduction of ligand's binaphthyl core[55] or the change of the amino group to imine fragment[56] allowed the formation of *P,N*-coordination to the palladium center, consistent with the expectation for a more basic nitrogen donor (Figure 2B). Furthermore, a recent study confirmed again that

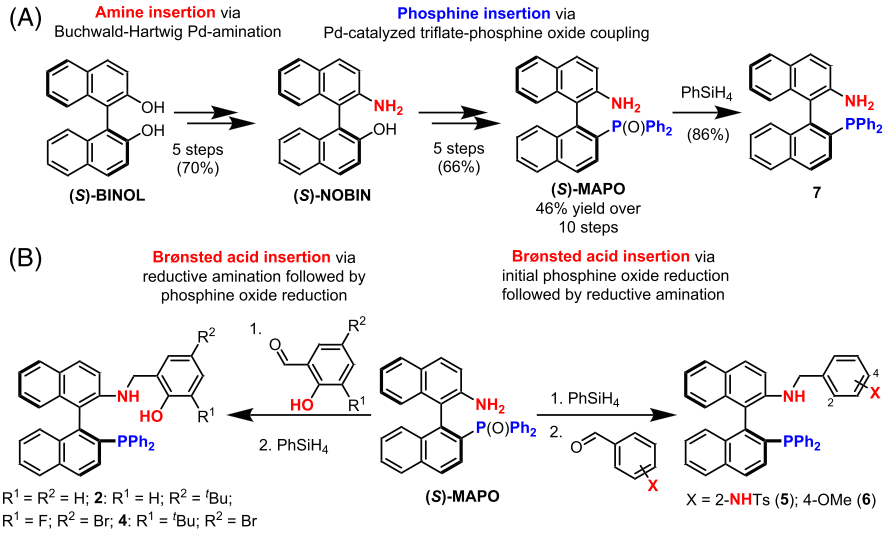

SCHEME 1 Synthesis of ligands **1**–**6**

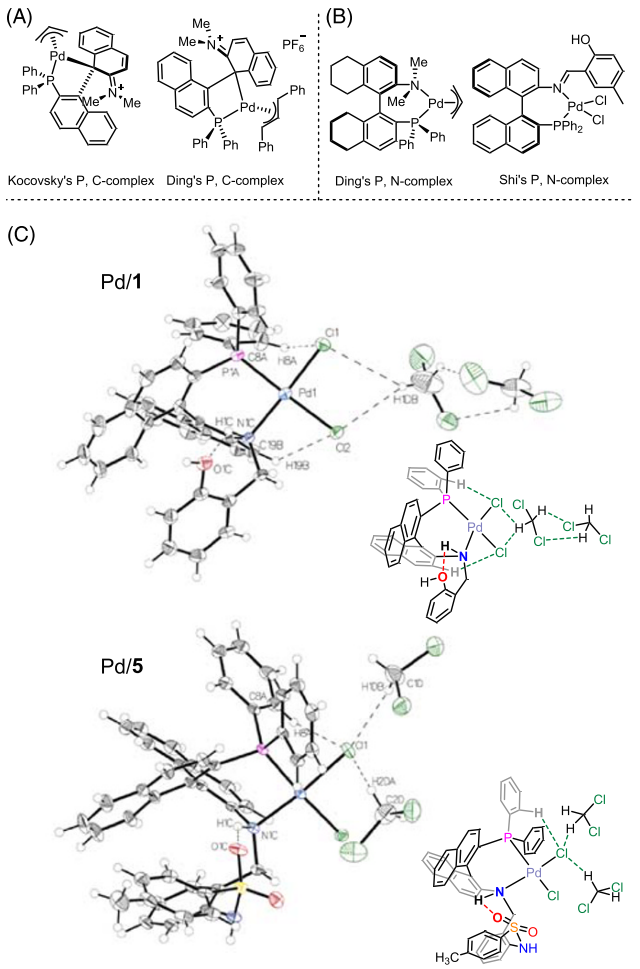

FIGURE 2 (A) MAP complexes with P,C_σ-coordination mode of palladium,[54,55] (B) modified MAP ligands in *P,N*-complexes with palladium,[55,56] and (c) ORTEP drawings of Pd/**1** and Pd/**5** complexes with hydrogen and halogen bond networks

unreduced binaphthyl-containing aminophosphines tend to form the Pd complex in the P,C_σ-coordination mode.[57]

The structure of palladium complexes of multifunctional ligands **1** and **5** was investigated by X-Ray crystallography (Figure 2C). The complexes Pd/**1** and Pd/**5** were synthesized by equimolar addition of bis(benzonitrile) palladium (II) chloride to a corresponding ligand in dichloromethane at room temperature (NMR spectra and X-Ray details of complexes Pd/1 and Pd/5are provided in Supporting Information).

The X-ray investigation showed a *P,N*-coordination pattern of palladium in Pd/**1** and Pd/**5** that is novel for unreduced binaphthyl-containing aminophosphines. The crystal structures have also revealed the ability of ligands **1** and **5** to form hydrogen bond networks. Ligand **1** provides the hydrogen bond using the phenolic oxygen and the hydrogen of the *exo*-amino group that is ligated to the metal. Ligand **5** forms a different type of hydrogen bonding. The sulfonamide group (a different Brønsted acid compared with the phenol in Pd/**1**) in Pd/**5** demonstrated H-bonding interaction between one of the sulfonyl oxygen atoms and again the *exo*-amino group that is ligated to palladium. In both cases, the nitrogen coordinated to the palladium center is shown to be involved in H-bonding network, suggesting that the H-bonding interactions from the ligand may influence the ligand–metal coordination interactions. This novel complex type, in which the palladium coordination site is also part of an H-bonding network through a ligating protic motif, can provide a new donor-type metal–ligand–substrate strategy for potentially cooperative catalysis (Figure 1C). Both complexes Pd/**1** and Pd/**5** also showed the ability to form halogen bond networks between two dichloromethane molecules and aromatic hydrogens (H8A, H19B for Pd/**1** and H8A for Pd/**5**) through chlorine atoms of the complexes (Figure 2C).

3.3 | Pd-catalyzed asymmetric allylic substitution: Suppression of elimination competition

Symmetrically disubstituted allyl precursor 1,3-diphenyl-2-propylacaetate **8** was chosen as a standard test case to avoid unnecessary regioselectivity complications. Dimethyl malonate was used as a classic representative of C-nucleophiles for model allylic alkylation of acetate **8**. Diethyl zinc was reported to promote enantiomeric excess in AAA for biindane-based diphosphine ligands[58] and therefore tested along with *N,O*-bis(trimethylsilyl)acetamide (BSA). Ligand **1** with unsubstituted phenolic fragment was chosen as a model for the initial optimization process. It was initially tested in dry 1,4-dioxane but demonstrated only 7% conversion to the desired diester **9** over 48 h, while the unexpected reduction side product **10** was detected in 82% conversion (Scheme 2, Conditions 1).

Such palladium-catalyzed reduction of allyl acetates in the presence of alkyl zinc reagents, containing β-hydrogens, has been reported previously.[59] The formation of the reduction side product **10** in AAA conditions,

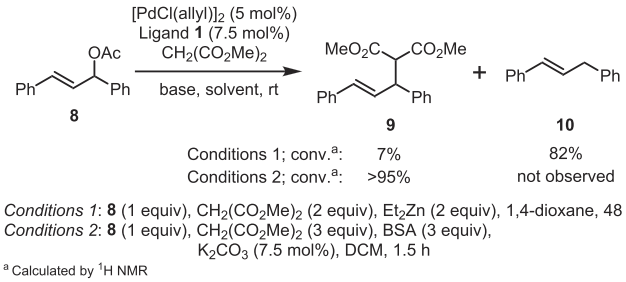

SCHEME 2 Initial test of ligand **1** in different asymmetric allylic alkylation (AAA) conditions

containing diethyl zinc as a base, was also reported for binaphthyl-based[60] and nicotine-based[61] monophosphine ligands but not for diphosphine ligands. This diethyl zinc interruption of the process probably occurs due to more weakly coordinated palladium-allyl intermediate with monophosphines compared with that from diphosphines. The use of another model Trost's AAA conditions,[62] where BSA was used instead of diethyl zinc as a malonate activator, afforded the formation of desired alkylation product **9** selectively over 1.5 h in 73: 27 *er* as predominantly the *R*-isomer (assigned by analogy with reference[63]) (Scheme 2, Conditions 2).

The enantioselectivity of the AAA reaction is known[53,56,64–68] to be influenced by base choice or loading and therefore was also investigated by changing these two parameters in an AAA test reaction with **1** as the ligand (Table 1). The potassium carbonate loading did not alter the enantioselectivity of reaction (Table 1, Entries 1–3). However, the decreased loading from 7.5 to 5 mol% reduced the reaction rate, providing 70% conversion to **9** at 1.5 h (Table 1, Entry 2 vs. Entry 1). The equimolar to substrate loading of BSA also led to a decline of the reaction rate to 61–69% conversion over 1.5 h without change in enantioselectivity (Table 1, Entries 4 and 5 vs. Entry 2). The use of potassium acetate instead of potassium carbonate allowed increasing the reaction rate and afforded >95% conversion over 0.5 h, albeit with little change in enantioselectivity (Table 1, Entry 6 vs. Entry 2). A previous report of AAA with MAP-based ligands showed enantioselectivity improvement at lower temperatures.[56] However, in our case, the AAA at 0°C led to a significant reaction rate decline with little difference in *er* (Table 1, Entry 7 vs. Entry 6). Further decrease of reaction temperature to −25°C decreased the rate further to a negligible level, providing **9** in only 10% conversion over 48 h (Table 1, Entry 8). Thus, the most practical conditions for monitoring the model AAA reaction were performed with 7.5 mol% loading of potassium carbonate and 3 equivalents of BSA as the dimethyl malonate activator at room temperature.

3.4 | Pd-catalyzed asymmetric allylic substitution: Enantiodivergent catalysis

Classic AAA reactions proceed through a symmetrical Pd-allyl intermediate that present as "M" and "W" isomers in rapid equilibrium (Figure 3A, left panel).[69,70] The M and W isomers interconvert readily even at temperatures below 0[71,72]; however, the ratio can be controlled by ligands with bulky substituents, disfavoring the formation of the W isomers that position the terminal phenyl group of the allyl intermediate closer to the bulkier ligand (Figure 3A, right panel).[73–75] In the case of the *P*,*N*-ligands investigated here, it is likely that the M isomer may be favored with the phosphorous center being the ligand side with bulkier substituents (Figure 3B). The following attack by a nucleophilic species can further contribute to the selectivity because of electronic factors, as the nucleophilic attack tends to prefer the allyl carbon *trans* to the better π-accepting phosphorous ligating atom (Figure 3B, Paths a and c preferred over Paths b and d).[76–78] Given that the enantioselectivity of the reaction is a complex outcome of multiple factors/pathways, ligands **1**–**6** were tested in a model AAA reaction in order to ascertain how the rate and enantioselectivity of the reaction may respond to the overall steric and electronic environment provided by these ligands.

TABLE 1 Reaction temperature and base additive loading tests

Entry	Base (loading), (mol%)	BSA (equiv)	Time (h)	Conv[a] [%]	*R:S er*[b]
1	K_2CO_3 (5)	3	1.5	70 (>95)[e]	72:28
2	K_2CO_3 (7.5)	3	0.5	30 (>95)[f]	73:27
3	K_2CO_3 (10)	3	1.5	>95	73: 27
4	K_2CO_3 (7.5)	1.05	1.5	69 (>95)[g]	72: 28
5	K_2CO_3 (7.5)	1.05	1.5	61 (>95)[g]	72: 28
6	KOAc (7.5)	3	0.5	>95	71: 29
7[c]	KOAc (7.5)	3	6	67 (>95)[g]	73: 27
8[d]	KOAc (7.5)	3	48	10	n.d.

[a]Calculated by ^{1}H NMR spectroscopy.
[b]Determined by HPLC analysis.
[c]Reaction at 0°C.
[d]Reaction at −25°C.
[e]3 h of reaction.
[f]1.5 h of reaction.
[g]24 h of reaction.

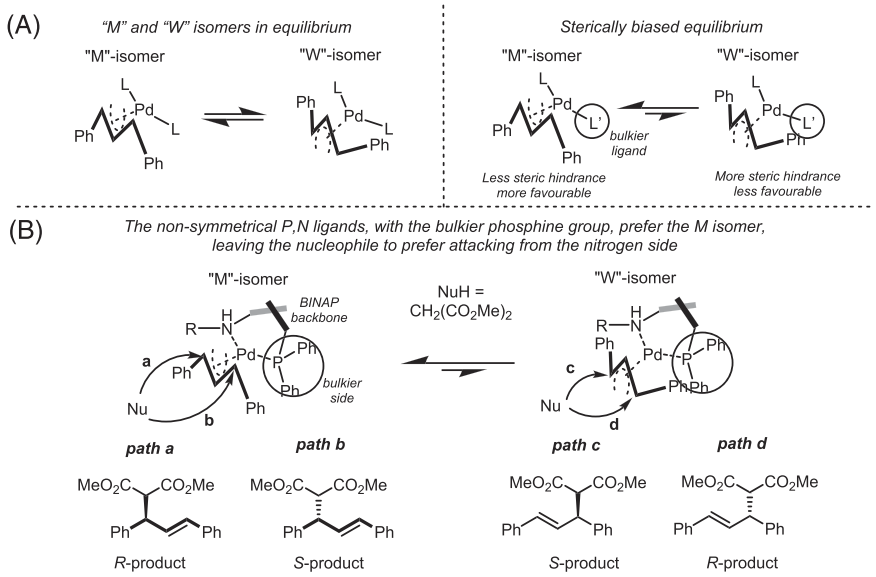

FIGURE 3 (A) Factors influencing "M" and "W" Pd-allyl isomer ratio in the AAA and (b) anticipated pathways leading to the *R* and *S* products in the AAA catalyzed by the chiral phosphine *P*,*N*-ligand system

Using the optimal condition for the model AAA reaction as investigated earlier, the conversion and enantiomeric ratios of the AAA between acetate **8** and dimethyl malonate were monitored for 1 h (Figure 4). Overall, these ligands showed fast conversion of reaction (1–6 h for complete conversion) with moderate enantiomeric ratios (62:38 to 18:82) and enantiodivergent catalysis (e.g., ligand **3** preferring the *R* product vs. ligand **5** preferring the *S* product). Ligands **2** and **3**, containing phenolic fragments with altered acidities compared to that of ligand **1**, demonstrated small variations in enantioselectivity, albeit with more significant differences on the reaction rate for ligand **3** (Figure 4, ligands **2** and **3** vs. ligand **1**). Ligand **3**, containing a fluorine substituent *ortho* to the phenol OH group, demonstrated a lower reaction rate than that by ligand **1** or **2** without any *ortho*-substituent (Figure 4, ligand **3** vs. ligands **1** and **2**). However, the reaction rate of ligand **3** was still faster than that for ligand **4**, suggesting that a bulky *ortho-tert*-butyl fragment would drastically reduce the reaction rate, providing full conversion to the desired product **9** only after 6 h (Figure 4, ligand **3** vs. ligand **4**). Furthermore, the sense of the asymmetric induction switched from preferring *R* for ligand **3** to *S* for ligand **4**. Ligand **5**, bearing a different tosylamide Brønsted acid, also exhibited a switch of the sense of the asymmetric induction from *R* to *S*, as compared with ligand **3** (Figure 4, ligand **5** vs. ligand **3**), although the rate of conversion for ligand **5** was faster than that of ligands **3** and **4** and close to that of ligands **1** and **2**. As a control without a phenol motif, ligand **6** demonstrated significant loss of reactivity providing only traces of product **9** over 1 h, with the sense and level of the asymmetric induction similar to that of ligand **2** (Figure 4, ligand **6**).

The relatively fast reaction rate, such as that from ligand **1** (>95% over 1.5 h) compared with previously

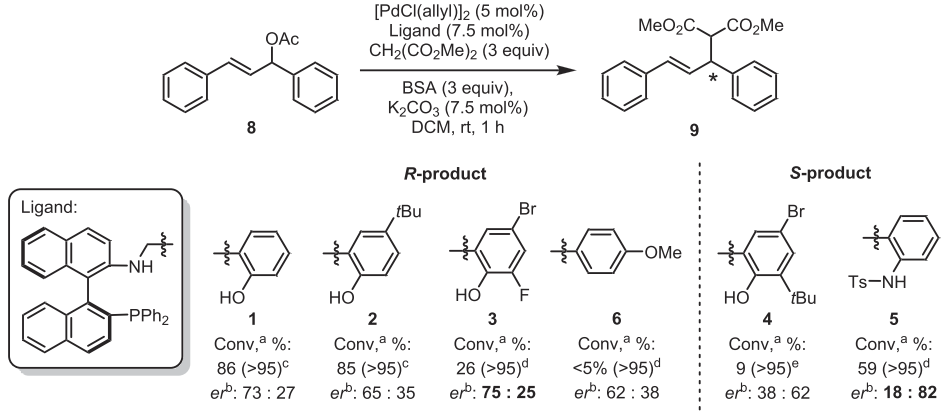

a Calculated by ^{1}H NMR spectroscopy. b Determined by HPLC analysis.
c 1.5 h of reaction. d 3 h of reaction. e 6 h of reaction.

FIGURE 4 Ligands **1–6** used in a model Pd-catalyzed asymmetric allylic alkylation (AAA)

reported MAP-based ligands[79–82] (>95% conversion over 6–48 h), suggests that this type of *P*,*N*-ligands may have different activation modes and potential for further development. The enantiodivergent catalysis from this series, along with the X-ray structural insight, also assisted in hypothesizing on the possible transition structures that may explain the observed reaction outcomes controlled by the complex outcomes of multiple pathways (Figure 3B, Paths a–d). The fast reaction rate can be attributed to a possible hydrogen-bonding interaction between ligand **1** (or a comparable ligand **2**) and the nucleophile (Figure 5A). The dramatic reduction of reaction rate provided by control ligand **6** supports the hypothesis of H-bonding activation from the ligand on the reaction rate. However, the moderate *R*-enantioselectivity and high reaction rate of Pd-catalyzed AAA provided by ligand **1** may require consideration of not just the H-bonding capacity of the ligand but also the steric environment in which the H-bonding interactions can be organized. As discussed earlier, preference for the M over the W isomer for the geometry of the Pd-allyl intermediate can be achieved by steric biasing with a bulkier phosphine group for ligation, along with the favorable nucleophile approach *trans* to the better π-accepting phosphorous ligating atom (Figure 3B, Path a), to prefer the *R* product. The low to moderate enantiomeric ratio of product **9** in this series suggests that in this model, the bias for the M isomer over the W isomer is likely also moderate and possibly prone to alteration of other steric factors also come into play.

The moderate reduction of reaction rate in the case of ligand **3**, compared with that of ligands **1** and **2**, may be due to the change in Brønsted acidity and also in the position of the phenolic hydrogen with an *ortho* fluorine substitution. However, the sense and level of the asymmetric induction were not significantly altered and still preferred the *R* product. As the steric bulk around the phenol increased in the case of ligand **4**, the sense of the asymmetric induction was switched to slightly prefer the *S* product, along with a large reduction in the conversion, suggesting the preclusion of H-bonding activation by the steric hindrance in the preferred *trans* nucleophilic approach and also consequentially higher preference for the *cis* approach in both the M and W isomer cases. Ligand **5** delivered a reaction rate comparable with that of ligand 1, while significantly altering the sense of the asymmetric induction to prefer the *S* product. (HPLC traces of product 9 are provided in Supporting Information). This enantiodivergence can be most consistently explained by a switched preference for the W isomer over the M isomer (Figure 5B), because of the large tosylsulfonamide group in closer proximity to the allyl substrate, a supposition consistent with the structural features shown by the X-ray analysis (Figure 2). While the H-bonding interactions between the tosyl NH and the nucleophile would still enhance the reaction rate and prefer the *trans* nucleophilic approach, the switched M/W preference would favor the *S* product overall. Effectively, enantiodivergent catalysis would be possible without changing the ligand chirality,

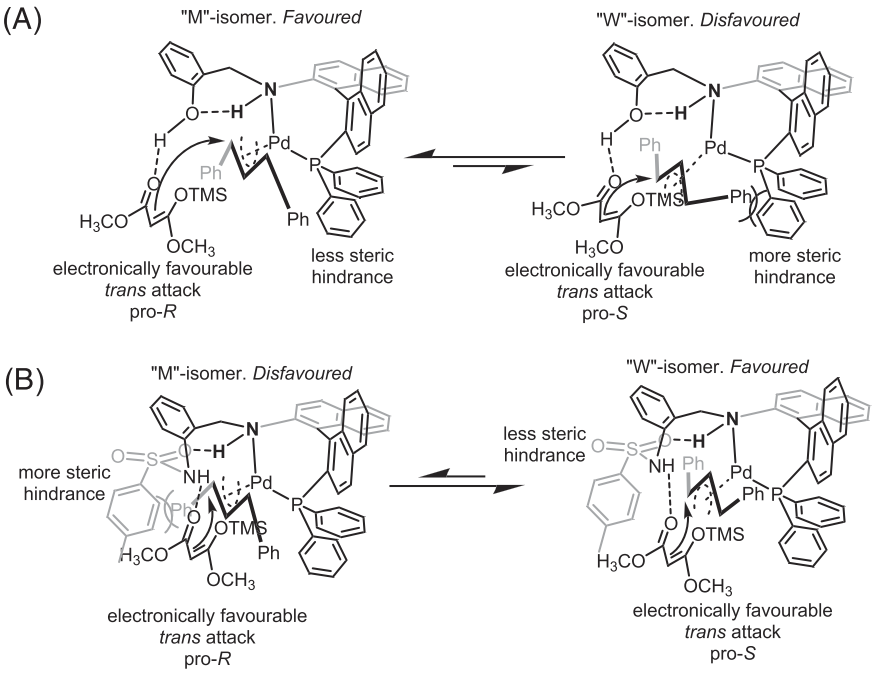

FIGURE 5 Proposed transition structures for ligands (A) **1** and (B) **5**

by altering the coordination between the various types of noncovalent interactions such as H-bonding interactions and steric hindrance in this series of multifunctional *P*,*N*-ligands.

4 | CONCLUSION

In summary, the ability of MAP-based, multifunctional chiral phosphines **1–6** to serve as ligands in model palladium-catalyzed AAA was demonstrated. Crystals of ligands **1** and **5** as palladium complexes were investigated by X-ray analysis and demonstrated an unusual *P*,*N*-coordination mode. The model reaction with the symmetrical AAA substrate **8** reveals the complexity behind the organized catalysis provided by multifunctional ligands **1–6**. The ligands in general promoted fast AAA reactions suggesting potential H-bonding activation in a donor-type metal–ligand–substrate strategy, with the ligand's Brønsted acid motif serving as a hydrogen bond donor for recruiting the nucleophile. The switch of the sense of the asymmetric induction to changing the ligand's Brønsted acid, without ligand chirality change, can be attributed to noncovalent interactions that alter H-bonding interactions between the ligand and the nucleophile as well as the bias for the preferred geometry of the metal–ligand–allyl complex. Thus, the ligand's set axial chirality in coordination with noncovalent interactions organized by the ligand's Brønsted acid motif between the metal, ligand, and substrates can lead to enantiodivergent catalysis by tuning both the H-bonding motif and its associated steric environment. Future work will involve tuning this type of ligands for further investigation of this model of organized noncovalent interactions in dynamic chirality translation with substrate scope and mechanistic analysis.

ACKNOWLEDGMENT

We are grateful to Macquarie University for an iMQRES scholarship (2015071) to Sviatoslav S. Eliseenko.

ORCID

Sviatoslav S. Eliseenko https://orcid.org/0000-0002-3230-8857

Fei Liu https://orcid.org/0000-0002-2175-6670

REFERENCES

1. Beletskaya IP, Nájera C, Yus M. Stereodivergent catalysis. *Chem Rev*. 2018;118(10):5080-5200.
2. Afewerki S, Córdova A. Enamine/transition metal combined catalysis: catalytic transformations involving organometallic electrophilic intermediates. *Top Curr Chem*. 2019;377(6):1-38.
3. Du Z, Shao Z. Combining transition metal catalysis and organocatalysis—an update. *Chem Soc Rev*. 2013;42(3):1337-1378.
4. Zhou Q-L. Transition-metal catalysis and organocatalysis: where can progress be expected? *Angew Chem Int Ed*. 2016;55(18):5352-5353.
5. Chen Z, Huo Y, An P, Wang X, Song C, Ma Y. [2.2]Paracyclophane-based *N*-heterocyclic carbene as efficient catalyst or as ligand for copper catalyst for asymmetric α-silylation of *N*-tosylaldimines. *Org Chem Front*. 2016;3(12):1725-1737.
6. Wang L, Chen Z, Ma M, Duan W, Song C, Ma Y. Synthesis and application of a dual chiral [2.2]paracyclophane-based *N*-heterocyclic carbene in enantioselective β-boration of acyclic enones. *Org Biomol Chem*. 2015;13(43):10691-10698.
7. Hernández-Rodríguez M, Avila-Ortiz CG, del Campo JM, Hernández-Romero D, Rosales-Hoz MJ, Juaristi E. Synthesis of novel chiral (thio)ureas and their application as organocatalysts and ligands in asymmetric synthesis. *Aust J Chem*. 2008;61(5):364-375.
8. Dahlin N, Bøgevig A, Adolfsson H. *N*-Arenesulfonyl-2-aminomethylpyrrolidines: novel modular ligands and organocatalysts for asymmetric catalysis. *Adv Synth Catal*. 2004;346(9–10):1101-1105.
9. Liu X, Lin L, Feng X. Chiral *N*,*N*′-dioxides: new ligands and organocatalysts for catalytic asymmetric reactions. *Acc Chem Res*. 2011;44(8):574-587.
10. Ni H, Tang X, Zheng W, Yao W, Ullah N, Lu Y. enantioselective phosphine-catalyzed formal [4 + 4] annulation of α,β-unsaturated imines and allene ketones: construction of eight-membered rings. *Angew Chem Int Ed*. 2017;56(45):14222-14226.
11. Krauss IJ, Leighton JL. Highly practical and enantioselective cu-catalyzed conjugate addition of alkylzinc reagents to cyclic enones at ambient temperature. *Org Lett*. 2003;5(18):3201-3203.
12. Albrecht A, Skrzyńska A, Przydacz A, Albrecht Ł. Nucleophilic catalysis in the enantioselective synthesis of α-methylidene-δ-lactones. *Synlett*. 2015;26(19):2679-2684.
13. Takizawa S, Nguyen TM-N, Grossmann A, Suzuki M, Enders D, Sasai H. Facile synthesis of α-methylidene-γ-butyrolactones: intramolecular Rauhut–Currier reaction promoted by chiral acid–base organocatalysts. *Tetrahedron*. 2013;69(3):1202-1209.
14. Takizawa S, Nguyen TM-N, Grossmann A, Enders D, Sasai H. Enantioselective synthesis of α-alkylidene-γ-butyrolactones: intramolecular Rauhut–Currier reaction promoted by acid/base organocatalysts. *Angew Chem Int Ed*. 2012;51(22):5423-5426.
15. Gong J-J, Li T-Z, Pan K, Wu X-Y. Enantioselective intramolecular Rauhut–Currier reaction catalyzed by chiral phosphinothiourea. *Chem Commun*. 2011;47(5):1491-1493.
16. Zhong F, Wang Y, Han X, Huang K-W, Lu Y. l-Threonine-derived novel bifunctional phosphine–sulfonamide catalyst-promoted enantioselective aza-Morita–Baylis–Hillman reaction. *Org Lett*. 2011;13(6):1310-1313.
17. Han X, Wang Y, Zhong F, Lu Y. Enantioselective Morita–Baylis–Hillman reaction promoted by l-threonine-derived

phosphine–thiourea catalysts. *Org Biomol Chem*. 2011;9(19):6734-6740.
18. Takizawa S, Kishi K, Kusaba M, Jianfei B, Suzuki T, Sasai H. Facile synthesis of spirooxindoles via an enantioselective organocatalyzed sequential reaction of oxindoles with ynone. *Heterocycles*. 2017;95(2):761-767.
19. Li E, Huang Y. Phosphine-catalyzed domino reactions: a route to functionalized bicyclic skeletons. *Chem A Eur J*. 2014;20(12):3520-3527.
20. Jin Z, Yang R, Du Y, Tiwari B, Ganguly R, Chi YR. Enantioselective intramolecular formal [2 + 4] annulation of acrylates and α,β-unsaturated imines catalyzed by amino acid derived phosphines. *Org Lett*. 2012;14(12):3226-3229.
21. Dilek Ö, Tezeren MA, Tilki T, Ertürk E. Chiral 2-(2-hydroxyaryl)alcohols (HAROLs) with a 1,4-diol scaffold as a new family of ligands and organocatalysts. *Tetrahedron*. 2018;74(2):268-286.
22. Théveau L, Bellini R, Dydio P, et al. Cofactor-controlled chirality of tropoisomeric ligand. *Organometallics*. 2016;35(11):1956-1963.
23. Höke T, Herdtweck E, Bach T. Hydrogen-bond mediated regio- and enantioselectivity in a C–H amination reaction catalysed by a supramolecular Rh (II) complex. *Chem Commun*. 2013;49(73):8009-8011.
24. Hayashi T, Kanehira K, Hagihara T, Kumada M. Asymmetric synthesis catalyzed by chiral ferrocenylphosphine-transition metal complexes. 5. Palladium-catalyzed asymmetric allylation of active methine compounds. *J Org Chem*. 1988;53(1):113-120.
25. Hayashi T, Yamamoto A, Ito Y, Nishioka E, Miura H, Yanagi K. Asymmetric synthesis catalyzed by chiral ferrocenylphosphine - transition-metal complexes. 8. Palladium-catalyzed asymmetric allylic amination. *J Am Chem Soc*. 1989;111(16):6301-6311.
26. Hayashi T, Kishi K, Yamamoto A, Ito Y. Asymmetric allylic amination catalyzed by chiral ferrocenylphosphine-palladium complexes. *Tetrahedron Lett*. 1990;31(12):1743-1746.
27. Hoarau O, Aït-Haddou H, Daran J-C, Cramailère D, Balavoine GGA. Asymmetric palladium-catalyzed allylic alkylation using Bis(oxazoline) ligands: phenomenal reversal of enantioselectivity with a single chiral backbone. *Organometallics*. 1999;18(23):4718-4723.
28. Aït-Haddou H, Hoarau O, Cramailére D, Pezet F, Daran J-C, Balavoine GGA. New dihydroxy Bis(oxazoline) ligands for the palladium-catalyzed asymmetric allylic alkylation: experimental investigations of the origin of the reversal of the enantioselectivity. *Chem A Eur J*. 2004;10(3):699-707.
29. Voss F, Herdtweck E, Bach T. Hydrogen bond induced enantioselectivity in Mn (salen)-catalysed sulfoxidaton reactions. *Chem Commun*. 2011;47(7):2137-2139.
30. Fackler P, Huber SM, Bach T. Enantio- and regioselective epoxidation of olefinic double bonds in quinolones, pyridones, and amides catalyzed by a ruthenium porphyrin catalyst with a hydrogen bonding site. *J Am Chem Soc*. 2012;134(30):12869-12878.
31. Huang Z, Lim LH, Chen Z, et al. Arene CH—O hydrogen bonding: a stereocontrolling tool in palladium-catalyzed arylation and vinylation of ketones. *Angew Chem Int Ed*. 2013;52(18):4906-4911.
32. Huang Z, Chen Z, Lim LH, Quang GCP, Hirao H, Zhou J. Weak arene C—H¨¨O hydrogen bonding in palladium-catalyzed arylation and vinylation of lactones. *Angew Chem Int Ed*. 2013;52(22):5807-5812.
33. Wen J, Fan X, Tan R, et al. Brønsted-acid-promoted Rh-catalyzed asymmetric hydrogenation of *N*-unprotected indoles: a cocatalysis of transition metal and anion binding. *Org Lett*. 2018;20(8):2143-2147.
34. Liu G, Han Z, Dong X-Q, Zhang X. Rh-catalyzed asymmetric hydrogenation of β-substituted-β-thio-α,β-unsaturated esters: expeditious access to chiral organic sulfides. *Org Lett*. 2018;20(18):5636-5639.
35. Wen J, Jiang J, Zhang X. Rhodium-catalyzed asymmetric hydrogenation of α,β-unsaturated carbonyl compounds via thiourea hydrogen bonding. *Org Lett*. 2016;18(18):4451-4453.
36. Li P, Zhou M, Zhao Q, et al. Synthesis of chiral β-amino nitroalkanes via rhodium-catalyzed asymmetric hydrogenation. *Org Lett*. 2016;18(1):40-43.
37. Zhao Q, Li S, Huang K, Wang R, Zhang X. A novel chiral bisphosphine-thiourea ligand for asymmetric hydrogenation of β,β-disubstituted nitroalkenes. *Org Lett*. 2013;15(15):4014-4017.
38. Corey EJ, Lee TW. The formyl C–H···O hydrogen bond as a critical factor in enantioselective Lewis-acid catalyzed reactions of aldehydes. *Chem Commun*. 2001;15:1321-1329.
39. Marshall JA, Palovich MR. Enantioselective and diastereoselective additions of allylic stannanes to aldehydes promoted by a chiral (acyloxy)borane catalyst. *J Org Chem*. 1998;63(13):4381-4384.
40. Paton RS, Goodman JM. 1,5-anti stereocontrol in the boron-mediated aldol reactions of β-alkoxy methyl ketones: the role of the formyl hydrogen bond. *J Org Chem*. 2008;73(4):1253-1263.
41. Eliseenko SS, Liu F. Switchable pyrrole-based hydrogen bonding motif in enantioselective trifunctional organocatalysis. *Tetrahedron*. 2019;75(4):518-526.
42. Kenny R, Liu F. Cooperative trifunctional organocatalysts for proficient proton transfer reactions. *Chem Rec*. 2017;17(5):535-553.
43. Liu F. The upside of downsizing: asymmetric trifunctional organocatalysts as small enzyme mimics for cooperative enhancement of both rate and enantioselectivity with regulation. *Chirality*. 2013;25(11):675-683.
44. Anstiss C, Karuso P, Richardson M, Liu F. Synthesis of new BINAP-based aminophosphines and their 31P-NMR spectroscopy. *Molecules*. 2013;18(3):2788–2802.
45. Anstiss C, Liu F. Cooperativity in the counterion catalysis of Morita/Baylis/Hillman reactions promoted by enantioselective trifunctional organocatalysts. *Tetrahedron*. 2010;66(29):5486-5491.
46. Anstiss C, Garnier J-M, Liu F. Mechanistic investigations of multidentate organocatalyst-promoted counterion catalysis for fast and enantioselective aza-Morita-Baylis-Hillman reactions at ambient temperature. *Org Biomol Chem*. 2010;8(19):4400-4407.
47. Garnier J-M, Liu F. Trifunctional organocatalyst-promoted counterion catalysis for fast and enantioselective aza-Morita-Baylis-Hillman reactions at ambient temperature. *Org Biomol Chem*. 2009;7(7):1272-1275.

48. Garnier J-M, Anstiss C, Liu F. Enantioselective trifunctional organocatalysts for rate- enhanced aza-morita–baylis–hillman reactions at room temperature. *Adv Synth Catal*. 2009;351(3): 331-338.
49. Alegre-Requena JV, Marqués-López E, Herrera RP. Optimizing the accuracy and computational cost in theoretical squaramide catalysis: the Henry reaction. *Chem A Eur J*. 2017;23(61):15336-15347.
50. Alegre-Requena JV, Marqués-López E, Herrera RP. "Push–Pull π+/π–" (PPππ) Systems in Catalysis. *ACS Catal*. 2017;7(10): 6430-6439.
51. Alegre-Requena JV, Marqués-López E, Herrera RP. Trifunctional squaramide catalyst for efficient enantioselective henry reaction activation. *Adv Synth Catal*. 2016;358(11):1801-1809.
52. Armarego WLF, Chai CLL. *Purification of Laboratory Chemicals*. 6th ed. Burlington: Butterworth-Heinemann; 2009: 1-743.
53. Watson IDG, Yudin AK. New insights into the mechanism of palladium-catalyzed allylic amination. *J Am Chem Soc*. 2005; 127(49):17516-17529.
54. Kočovský P, Vyskočil Š, Císařová I, et al. Palladium (II) complexes of 2-dimethylamino-2′- diphenylphosphino-1,1′-binaphthyl (MAP) with unique P,C_σ-coordination and their catalytic activity in allylic substitution, Hartwig−Buchwald amination, and Suzuki coupling. *J Am Chem Soc*. 1999;121(33): 7714-7715.
55. Wang Y, Li X, Sun J, Ding K. Backbone effect of map ligands on their coordination patterns with palladium (II). *Organometallics*. 2003;22(9):1856-1862.
56. Sun Y-W, Jiang J-J, Zhao M-X, Wang F-J, Shi M. Palladium-catalyzed asymmetric allylic substitutions in the presence of chiral phosphine-imine type ligands. *J Organomet Chem*. 2011; 696(15–16):2850-2856.
57. Ding L, Sui X, Gu Z. Enantioselective synthesis of biaryl atropisomers via Pd/norbornene-catalyzed three-component cross-couplings. *ACS Catal*. 2018;8(6):5630-5635.
58. Xie J-H, Duan H-F, Fan B-M, Cheng X, Wang L-X, Zhou Q-L. Application of SDP ligands for Pd-catalyzed allylic alkylation. *Adv Synth Catal*. 2004;346(6):625-632.
59. Matsushita H, Negishi E. Palladium-catalyzed reactions of allylic electrophiles with organometallic reagents. A regioselective 1,4-elimination and a regio- and stereoselective reduction of allylic derivatives. *J Org Chem*. 1982;47(21):4161-4165.
60. Kinoshita N, Kawabata T, Tsubaki K, Bando M, Fuji K. Use of zinc enolate, free from other metals, in enantioselective palladium-catalyzed allylic alkylation. *Tetrahedron*. 2006;62(8): 1756-1763.
61. Comins DL, Capracotta SS. Nicotine-based compounds useful for asymmetric synthesis patent WO2010040059 (A1). 2010.
62. Trost BM, Murphy DJ. A model for metal-templated catalytic asymmetric induction via.pi.-allyl fragments. *Organometallics*. 1985;4(6):1143-1145.
63. Enders D, Peters R, Lochtman R, Runsink J. Enantioselective synthesis of planar chiral ortho-functionalized ferrocenyl ketones. *Eur J Org Chem*. 2000;16:2839-2850.
64. Long P-W, Xu J-X, Bai X-F, et al. Palladium-catalyzed tandem allylic substitution/cyclization and cascade hydrosilylated reduction: the influence of reaction parameters and hydrosilanes on the stereoselectivity. *RSC Adv*. 2018;8(41): 22944-22951.
65. Ghorpade SA, Sawant DN, Makki A, Sekar N, Eppinger J. Water promoted allylic nucleophilic substitution reactions of (*E*)-1,3 diphenylallyl acetate. *Green Chem*. 2018;20(2): 425-430.
66. Rovira L, Fernández-Pérez H, Vidal-Ferran A. Palladium-based supramolecularly regulated catalysts for asymmetric allylic substitutions. *Organometallics*. 2016;35(4):528-533.
67. Chen M, Hartwig JF. Iridium-catalyzed enantioselective allylic substitution of enol silanes from vinylogous esters and amides. *J Am Chem Soc*. 2015;137(43):13972-13979.
68. Lai Z-W, Yang R-F, Ye K-Y, Sun H, You S-L. Synthesis of 1-[bis (trifluoromethyl)phosphine]-1′-oxazolinylferrocene ligands and their application in regio- and enantioselective Pd-catalyzed allylic alkylation of monosubstituted allyl substrates. *Beilstein J Org Chem*. 2014;10:1261-1266.
69. Trost BM, Van Vranken DL. Asymmetric transition metal-catalyzed allylic alkylations. *Chem Rev*. 1996;96(1):395-422.
70. Guerrero Rios I, Rosas-Hernandez A, Martin E. Recent advances in the application of chiral phosphine ligands in Pd-catalysed asymmetric allylic alkylation. *Molecules*. 2011;16(1): 970-1010.
71. Sprinz J, Kiefer M, Helmchen G, et al. Catalysis of allylic substitutions by Pd complexes of oxazolines containing an additional P, S, or Se Center. X-ray crystal structures and solution structures of chiral π-allyl palladium complexes of phosphinoaryloxazolines. *Tetrahedron Lett*. 1994;35(10): 1523-1526.
72. Granberg KL, Baeckvall JE. Isomerization of (.pi.-allyl)palladium complexes via nucleophilic displacement by palladium (0). A common mechanism in palladium(0)-catalyzed allylic substitution. *J Am Chem Soc*. 1992;114(17):6858-6863.
73. Nakano H, Okuyama Y, Yanagida M, Hongo H. Palladium-catalyzed asymmetric allylic substitution reactions using new chiral phosphinooxathiane ligands. *J Org Chem*. 2001;66(2): 620-625.
74. Kraft J, Mill K, Ziegler T. Sugar-annulated oxazoline ligands: a novel Pd (II) Complex and its application in allylic substitution. *Molecules*. 2016;21(12):1704–1715.
75. Anderson JC, Cubbon RJ, Harling JD. Investigation of the importance of nitrogen substituents in a N–P chiral ligand for enantioselective allylic alkylation. *Tetrahedron: Asymmetry*. 2001;12(6):923-935.
76. Aakermark B, Hansson S, Krakenberger B, Vitagliano A, Zetterberg K. Alkylation of (.pi.-allyl)palladium systems. Mechanism and regiocontrol. *Organometallics*. 1984;3(5):679-682.
77. Dawson GJ, Williams JMJ, Coote SJ. Enantioselective synthesis of succinic acids and γ-lactones via palladium catalysed allylic substitution reactions. *Tetrahedron: Asymmetry*. 1995;6(10): 2535-2546.
78. Allen JV, Coote SJ, Dawson GJ, Frost CG, Martins CJ, Williams JMJ. Palladium-catalysed asymmetric allylic substitution: a ligand design incorporating steric and electronic effects. *J Chem Soc, Perkin Trans*. 1994;1(15):2065-2072.
79. Vyskočil Š, Smrčina M, Hanuš V, Polášek M, Kočovský P. Derivatives of 2-amino-2′-diphenylphosphino-1,1′-binaphthyl (MAP) and their application in asymmetric palladium(0)-

catalyzed allylic substitution. *J Org Chem*. 1998;63(22):7738-7748.
80. Wang Y, Guo H, Ding K. Synthesis of novel N,P chiral ligands for palladium-catalyzed asymmetric allylations: the effect of binaphthyl backbone on the enantioselectivity. *Tetrahedron: Asymmetry*. 2000;11(20):4153-4162.
81. Wang Y, Li X, Ding K. The synthesis of a new generation of MAP ligands containing two types of chiral elements for asymmetric catalysis. *Tetrahedron Lett*. 2002;43(1):159-161.
82. Kawamura M, Kiyotake R, Kudo K. Synthesis of a novel photoresponsive axially chiral phosphine ligand containing an arylazo group and its application to palladium-catalyzed asymmetric allylic alkylation. *Chirality*. 2002;14(9):724-726.

SUPPORTING INFORMATION

Additional supporting information may be found online in the Supporting Information section at the end of this article.

How to cite this article: Eliseenko SS, Bhadbhade M, Liu F. Multifunctional chiral aminophosphines for enantiodivergent catalysis in a palladium-catalyzed allylic alkylation reaction. *Chirality*. 2020;1–13. https://doi.org/10.1002/chir.23275